

## Interplay between magnetism and sodium vacancy ordering in $\text{Na}_x\text{CoO}_2$

S. Galeski,\* K. Mattenberger, and B. Batlogg

*Solid State Physics Laboratory, ETH Zurich, CH-8093 Zurich, Switzerland*

(Received 18 May 2016; revised manuscript received 6 September 2016; published 5 October 2016)

Using a combination of low-temperature nanocalorimetry and x-ray diffraction we identify three temperature regimes characterized by distinct Na ordering patterns (low temperature up to 290 K, intermediate 290–340 K, and high above 340 K). Through freezing-in of these patterns we establish the two key roles sodium intercalation plays in the formation of the magnetic ground state: supplying the proper electron count for in-plane ferromagnetic interaction and through the 3D sodium ordering providing the interplane antiferromagnetic exchange path.

DOI: [10.1103/PhysRevB.94.140402](https://doi.org/10.1103/PhysRevB.94.140402)

When first synthesized  $\text{Na}_x\text{CoO}_2$  was considered a good candidate material for manufacturing rechargeable battery electrodes, yet it soon became clear that due to its higher ion mobility  $\text{Li}_x\text{CoO}_2$  would be the preferred material in energy storage. However because of the low abundance of lithium in the earth's crust and the high costs of its extraction  $\text{Na}_x\text{CoO}_2$  has again attracted interest as a simplest possible alternative.

While Na acts as a charge reservoir in  $\text{Na}_x\text{CoO}_2$  battery electrodes its role in defining the complex physical properties immanent to the  $\text{CoO}_2$  layers is much more subtle. Na tends to order and thus provides a complex Coulomb potential landscape acting upon the cobalt  $3d$  orbitals. This together with the highly correlated character of the electrons in the  $\text{CoO}_2$  layers leads to the emergence of a plethora of collective electronic ground states, including charge, spin density waves, and even superconductivity when hydrated [1–6]. Moreover even in the regions of the phase diagram without any electronic ordering the properties of  $\text{Na}_x\text{CoO}_2$  can be very unusual. This is especially visible in the Curie-Weiss metal phase occurring for Na content just above the Lifshitz transition [7,8].

A central question in the discussion of  $\text{Na}_x\text{CoO}_2$  is whether all these Fermi surface instabilities originate from the change of electron count only or whether, for a given value of  $x$ , the geometric arrangement of Na ions plays an essential role for electronic ordering in the  $\text{CoO}_2$  layers [2,9,10].

A first hint comes from the comparison of phase diagrams of  $\text{Na}_x\text{CoO}_2$  with its sister compound  $\text{Li}_x\text{CoO}_2$ , the widely used electrode material due to its high Li mobility. Interestingly for the same electron count, the ground states are found to be different [11]. One possible reason for this difference could be the reduced ion mobility in  $\text{Na}_x\text{CoO}_2$  with the unique advantage of being slow enough to be accessible to experiments [12,13].

Another surprising phenomenon is that for certain sodium contents the low-temperature ordering is dependent on cooling history of the sample [14]. This raises the question about the cause of the history effect: Is it freezing-in of the high-temperature crystallographic structure or perhaps of the interlayer sodium superstructures?

In this study we show, by using a combination of calorimetry and x-ray diffraction (XRD), not only that the sodium superstructures are responsible for the thermal history effect but also which sodium superstructures induce particular

magnetic transitions. Moreover by rapid cooling (over 6000 K/s) we are able to freeze-in the most disordered sodium configuration proving that even short-range sodium correlations are sufficient to sustain low-temperature magnetic order.

The difficulty in comparing the low-temperature magnetic order with sodium superstructures lies in the fact that they can change upon cooling through the structural transitions of the underlying lattices making the magnetic structures that could rise due to high-temperature sodium ordering inaccessible in standard experiments [14]. To overcome this difficulty we have employed a membrane calorimeter (Xensor, Inc. [15]). With this setup samples as small as 10–100 ng could be measured and more importantly the temperature could be varied with heating and cooling rates up to 6000 K/s enabling us to effectively freeze-in the high-temperature Na structures. Such fast cooling rates were achieved by keeping the cryostat at 30 K and then passing a current pulse through one of the resistors on the sample stage. A typical thermal cycle curve is shown in Fig. 1.

The calorimetric measurements were performed using the  $3\omega$  method [16,17] and were cross-checked with standard measurements on large crystals from the same batch performed on the Quantum Design PPMS specific-heat option. The

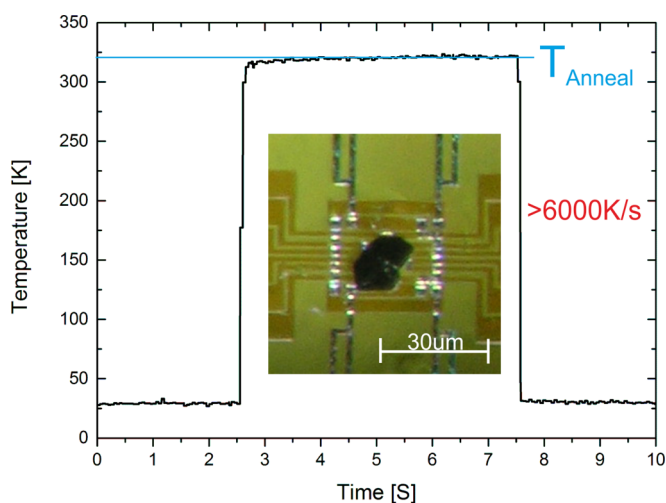


FIG. 1. A typical temperature profile to freeze-in the Na configuration established at the annealing temperature, by subsequent quenching at a rate faster than 6000 K/sec.

\*Corresponding author: [galeskis@phys.ethz.ch](mailto:galeskis@phys.ethz.ch)

crystals were grown by the floating zone method [18], and the sodium content was determined using the known relation between  $c$ -axis length and sodium concentration [14,19,20]. The crystal structure and the sodium superlattices were characterized using the in-house Bruker Apex SMART II single-crystal diffractometer equipped with an Oxford Instruments temperature control system.

In the following we present results of three experiments showing the relation between low-temperature magnetic ordering and high-temperature sodium ordering. In the first section quenching the sample from different high temperatures is shown to yield different low-temperature states. This is followed by a short discussion of sodium dynamics and how different sodium structures evolve from one into the other. As the last result we show x-ray Laue diffraction patterns directly relating different low-temperature magnetic states to certain high-temperature sodium states.

To establish the boundaries defining the relation between magnetism and sodium ordering in  $\text{Na}_{0.84}\text{CoO}_2$  we have performed a series of annealing experiments. The sample was initially slowly cooled (1 K/min) from 300 K to 30 K and then annealed for 5 seconds at successively higher temperatures with subsequent quenching back to 30 K for specific-heat measurements. Thanks to the fast cooling rates (over 6000 K/s; Fig. 1) a direct mapping was possible between sodium configurations characteristic for particular elevated temperatures and the low-temperature magnetic state they would induce in the  $\text{CoO}_2$  layers. Three distinct magnetic phases can be induced in the same  $\text{Na}_{0.84}\text{CoO}_2$  crystal by freezing-in different Na configurations (Fig. 2, left panel). When the sample is cooled down slowly or annealed at temperatures between where the temperature-activated sodium mobility becomes visible on the scale of minutes and 286 K, the magnetic state is characterized by two specific-heat peaks at 8 K and 21.5 K. On subsequent annealing at slightly higher temperatures the 8 K peak diminishes slowly and another begins to form at 15 K. This change coincides with the previously reported structural transition taking place at around 290 K; it separates the “low temperature” and “intermediate temperature” regions.

The magnetic order associated with the sodium structure above 336 K, the “high temperature” region, is yet different: all transitions previously reported [4,14] are suppressed and replaced by a single specific-heat anomaly at 23 K. We have annealed the sample up to 770 K and found no further modification of the low-temperature magnetic state.

In the same way we have also studied another composition:  $\text{Na}_{0.75}\text{CoO}_2$  and observed less spectacular changes in the low-temperature magnetism: a slight suppression of  $T_N$  for the sodium configuration in the 250–330 K range (Fig. 3).

To better understand the dynamics and evolution of sodium structures we have performed an annealing experiment in which the sample was prepared in the high-temperature state by quenching it from 425 K and then annealed for short periods of time at 180 K with its low-temperature specific heat probed between the annealing steps. At 180 K Na is barely mobile enough to rearrange to the equilibrium configuration after hours of annealing, so that transient magnetic states can be monitored precisely (Fig. 2, right panel).

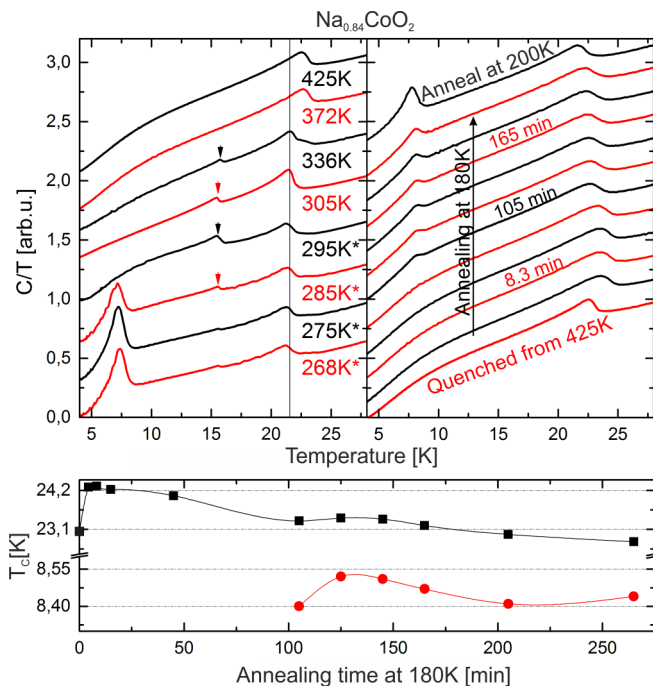


FIG. 2. Emergence of low-temperature magnetic state for two different quenching and annealing protocols (see text). Left panel: Specific-heat data taken after annealing the samples at indicated temperatures for 5 s. (The star indicates data from the second crystal; due to the extreme temperature gradients between the sample stage and the cryostat the SiN membranes occasionally broke. However the presented results were cross-checked on four other crystals from two batches and turned out to be fully reproducible.) Right panel: Evolution of the magnetic order with the change of sodium structure from most disordered to the low-temperature ordering. The sample was prepared by quenching from 425 K and then subsequently annealed at 180 K. Bottom panel: Transition temperature evolution as a function of annealing time.

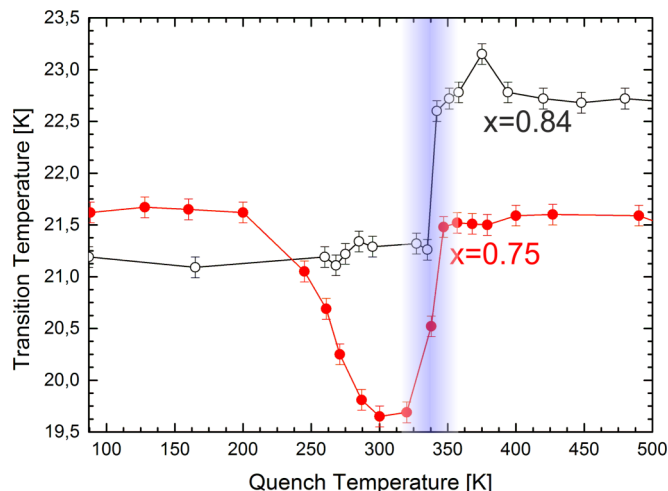


FIG. 3. Variation of the transition temperature of the highest temperature magnetic phase transition as a function of quenching temperature for two Na concentrations. The blue region indicates the location of the sodium lattice melting.

The most striking observation is that the 22 K and the 23 K peaks seem to be continuously connected. Except for the rapid change in the first 4 minutes of annealing, the shape of the specific-heat anomalies and the critical temperature vary very slowly (Fig. 2, bottom panel). Surprisingly this abrupt evolution increased the transition temperature to 24 K. One explanation of this phenomenon might be that in the first minutes of annealing the sodium atoms just move to the higher-symmetry position between the Co atoms [21] without moving far from the position they were frozen-in. This way the exchange slightly strengthens while maintaining the general high-temperature sodium structure.

More interestingly the 8 K magnetic state evolves from the 22 K in a direct way without the appearance of the “intermediate” 15 K peak. Furthermore once the 8 K phase starts to emerge its transition temperature evolves smoothly in direct correlation with the variations of the peak at 22–24 K (Fig. 2, bottom panel), suggesting that if there is any phase separation it will be on a scale short enough for both phases to interact.

After having established the three temperature regions associated with different magnetic order we searched for Na ordering patterns performing XRD experiments at temperatures between 260 K and 360 K on both  $x = 0.75$  and  $x = 0.84$  samples. Indeed we have found distinct superlattice reflections that are directly linked to these regions.

For  $x = 0.84$  below 290 K the Bragg peaks belonging to the  $\text{CoO}_2$  lattice are surrounded by superstructure reflections which form two “rings” of twined superstructures, as indicated in the upper row of Fig. 4. The superstructures can be indexed as tri- and divacancies ( $x = 11/13 = 0.8462$  and  $x = 16/19 = 0.8421$ , respectively), on a hexagonal lattice with unit vectors  $\sqrt{19}a$  and  $\sqrt{13}a$  rotated by  $2.5^\circ$  and  $15.9^\circ$  with respect to the original unit cell vectors. On crossing the 290 K structural phase transition the twin  $\sqrt{19}a$  reflections merge into a “hexagon of hexagons” pattern [22].

Even more pronounced changes occur above 335 K: a nearly complete disappearance of superstructure Bragg peaks. Although there seems to be a reminiscence of the hexagon-of-hexagons pattern its intensity is suppressed (Fig. 5, right third panel from the top). Instead of a series of sharp Bragg peaks a blurred halo develops around the main reflections. This is an indication of the melting of the sodium superstructure lattice, and a formation of what could be called a correlated sodium vacancy liquid: a state in which the sodium vacancy droplets are still present due to Coulomb repulsion but without angular ordering on the scale probed in an XRD experiment. At the same time the average sodium structure modulation length increases as best seen by comparison with the white circles.

An inspection of the  $1kl$  cuts of the reciprocal space reveals more details about the superstructures: Well-defined sodium ordering is present also along the  $c$  axis. In particular the trivacancy layers follow the periodicity of the crystal (red and green arrows). On the other hand the location of the divacancy peaks suggests an additional modulation tripling the original unit cell height in accordance with previous findings (blue arrows) [10].

Sodium superstructures for  $x = 0.75$  are slightly different: there is no detectable change on crossing 290 K, possibly due to resolution limitations of our setup: the crystallographic

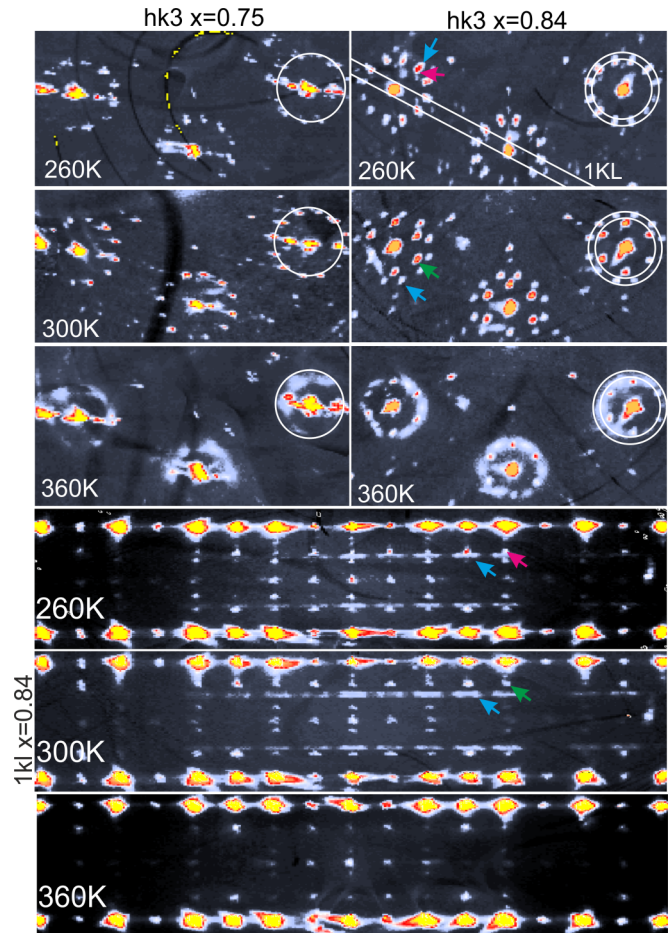


FIG. 4. In-plane and out-of-plane Na superstructures: X-ray diffraction patterns showing sodium superstructures characteristic for different temperatures. The images are  $hk3$  planes measured on a single crystal of  $\text{Na}_{0.84}\text{CoO}_2$  (right column) and  $\text{Na}_{0.75}\text{CoO}_2$  (left column). The white circles are a guide to the eye to visualize the change in modulation length. The white lines in the top right image indicate the integration range used for obtaining the  $1kl$  cuts. The colored arrows indicate reflections of distinct superstructures. The color code is maintained throughout this Rapid Communication ( $\sqrt{13}a$ , blue;  $\sqrt{19}a$ , purple;  $5a$ , green).

transition at 290 K is very subtle [13], thus the possible superstructure modification is expected to be minuscule. However melting of the sodium superstructures above is 335 K still present.

Figure 5 summarizes the salient features of the structure and heat capacity studies as a function of temperature: reflection intensities for various superlattice peaks, specific-heat peak heights for various magnetic orderings, and the specific-heat anomalies that mark the boundaries between the three discussed temperature regions.

The specific-heat anomaly around 280 K coincides with the known structural transition of the unit cell from orthorhombic to monoclinic. At this point it is not clear whether the 290 K peak is associated directly with the  $\text{CoO}_2$  lattice transition or with the sodium rearrangement.

No structural transitions of the  $\text{CoO}_2$  units were reported for the 335 K region [13]; however, neutron powder diffraction

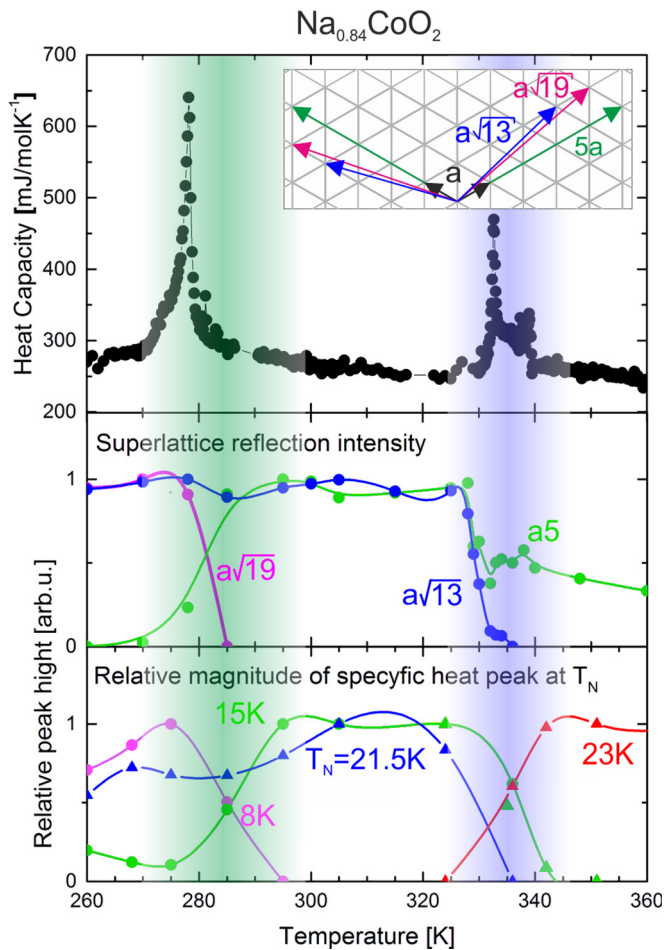


FIG. 5. Summary linking calorimetric and structural data measured on  $\text{Na}_{0.84}\text{CoO}_2$ . Top panel: High-temperature heat capacity. Middle panel: Normalized intensities of superstructure reflections taken from the images of the right panel, for the Laue diffraction patterns (see Supplemental Material [26]). Bottom panel: Relative magnitude of specific-heat anomalies.

studies suggested a movement of Na ions away from the most symmetric position in the Co triangles [21]. This supports the proposed emergence of a sodium vacancy liquid.

The central result of this study is shown in Fig. 5: the superlattice peak intensities and the specific-heat anomalies, signatures of magnetic states, are closely correlated. In particular the 8 K transition is related to the  $\sqrt{19}a$  superstructure which disappears at 290 K replaced by a  $5a$  superstructure pattern responsible for the magnetic order at 15 K.

This pattern as suggested by Morris *et al.* [22] could indicate the formation of disordered sodium vacancy stripes. These stripes would in a natural way lead to the modification of the effective dimensionality of the magnetic interactions, thus explaining the observed pronounced magnetic fluctuation tail preceding the 15 K transition [23].

On cooling the 290 K transition involves a locking in of the modulation direction to the prevalent  $\sqrt{13}a$  modulation. In order to stay commensurate with the  $\text{CoO}_2$  lattice the modulation length slightly decreases from  $5a$  to  $\sqrt{19}a$  (inset of Fig. 5).

The 335 K transition is of a different kind: there is no lattice structural transition and no transition between different superstructures. On crossing the transition temperature superstructure Bragg peaks fade away. Freezing-in of this disordered state could be pictured as creating a sodium vacancy glass and is associated with the disappearance of all so far known magnetically ordered phases and the emergence of a new state with transition temperature of 23 K and with a spin-flop transition [1] at 12 T (see Supplemental Material [26]), suggesting that the presence of sodium long-range order is not necessary for magnetism to develop.

Our studies show that  $\text{Na}_{0.84}\text{CoO}_2$  has a strong tendency towards A-type antiferromagnetism regardless of the details of the sodium arrangement. Due to the long wavelength of the sodium superstructure modulation and the overall hexagonal symmetry of the sodium patterns the itinerant-electron ferromagnetism in the  $\text{CoO}_2$  layers would not be significantly altered by modifications of sodium ordering. As was shown through measurements of the magnetic contribution to specific heat, magnetic fluctuations extend well beyond 50 K and thus any known 3D ordering temperature [24]. On the other hand it was shown by Johannes *et al.* [25] that the strength of the interplane interaction is very sensitive to the availability of exchange paths involving sodium  $sp^2$  orbitals. In particular the calculations predict the interaction strength to be 35% stronger if the sodium is placed directly under the Co atom [Na(1) position] instead of the center of the triangle made by the Co atoms [Na(2) position].

Our XRD results indicate that all the superstructures are well ordered along the  $c$  axis. This suggests that the reason for the occurrence of different transition temperatures is not the modification of the in-plane ferromagnetic fluctuations due to the Coulomb potential or a change of the stacking order of vacancies of different nature (di- or trivacancies) but the modification of the interplane coupling due to the change of relative location of vacancies in adjacent layers: the  $\sqrt{19}a$  and  $5a$  superstructures are both trivacancy patterns; however they induce different  $T_N$ 's.

In summary we have established the importance of 3D sodium ordering as a key ingredient influencing the electronic properties of  $\text{Na}_x\text{CoO}_2$ : (1) the sodium intercalation provides the proper electron count sustaining the in-plane ferromagnetism; (2) it mediates the antiferromagnetic exchange between the layers. This leads to a picture in which magnetism relies on the proper nesting and electron count as suggested by calculations of Kuroaki *et al.* [2] but the exact value of  $T_N$  is defined by the nature of sodium ordering.

Additionally we have shown that it is possible to freeze-in the disordered sodium vacancy liquid arrangement. This could allow us on one hand to obtain through electrochemical reactions at elevated temperatures samples of arbitrary sodium content, and on the other to investigate which phenomena are intrinsic to the  $\text{CoO}_2$  layers and which are emergent phenomena originating from the interplay of electronic degrees of freedom with the sodium order.

We would like to thank P. J. W. Moll, Y. Sassa, and J. Kanter for their input to this work and S. Gvasaliya for his assistance in performing the XRD experiments.

- [1] L. M. Helme, A. T. Boothroyd, R. Coldea, D. Prabhakaran, A. Stunault, G. J. McIntyre, and N. Kernavanois, *Phys. Rev. B* **73**, 054405 (2006).
- [2] K. Kuroki, S. Ohkubo, T. Nojima, R. Arita, S. Onari, and Y. Tanaka, *Phys. Rev. Lett.* **98**, 136401 (2007).
- [3] I. I. Mazin and M. D. Johannes, *Nat. Phys.* **1**, 91 (2005).
- [4] P. Mendels, D. Bono, J. Bobroff, G. Collin, D. Colson, N. Blanchard, H. Alloul, I. Mukhamedshin, F. Bert, A. Amato, and A. D. Hillier, *Phys. Rev. Lett.* **94**, 136403 (2005).
- [5] R. E. Schaak, T. Klimczuk, M. L. Foo, and R. J. Cava, *Nature (London)* **424**, 527 (2003).
- [6] K. Takada, H. Sakurai, E. Takayama-Muromachi, F. Izumi, R. A. Dilanian, and T. Sasaki, *Nature (London)* **422**, 53 (2003).
- [7] D. Yoshizumi, Y. Muraoka, Y. Okamoto, Y. Kiuchi, J.-I. Yamaura, M. Mochizuki, M. Ogata, and Z. Hiroi, *J. Phys. Soc. Jpn.* **76**, 063705 (2007).
- [8] Y. Wang, N. S. Rogado, R. J. Cava, and N. P. Ong, *Nature (London)* **423**, 425 (2003).
- [9] M. Roger, D. J. P. Morris, D. A. Tennant, M. J. Gutmann, J. P. Goff, J.-U. Hoffmann, R. Feyerherm, E. Dudzik, D. Prabhakaran, A. T. Boothroyd, N. Shannon, B. Lake, and P. P. Deen, *Nature (London)* **445**, 631 (2007).
- [10] G. J. Shu, F.-T. Huang, M.-W. Chu, J.-Y. Lin, P. A. Lee, and F. C. Chou, *Phys. Rev. B* **80**, 014117 (2009).
- [11] T. Motohashi, T. Ono, Y. Sugimoto, Y. Masubuchi, S. Kikkawa, R. Kanno, M. Karppinen, and H. Yamauchi, *Phys. Rev. B* **80**, 165114 (2009).
- [12] D. Carlier, M. Blangero, M. Menetrier, M. Pollet, J. P. Doumerc, and C. Delmas, *Inorg. Chem.* **48**, 7018 (2009).
- [13] M. Medarde, M. Mena, J. L. Gavilano, E. Pomjakushina, J. Sugiyama, K. Kamazawa, V. Y. Pomjakushin, D. Sheptyakov, B. Batlogg, H. R. Ott, M. Månsson, and F. Juranyi, *Phys. Rev. Lett.* **110**, 266401 (2013).
- [14] T. F. Schulze, P. S. Hafliger, C. Niedermayer, K. Mattenberger, S. Bubenhofer, and B. Batlogg, *Phys. Rev. Lett.* **100**, 026407 (2008).
- [15] S. van Herwaarden, Gas Nanocalorimeters, XEN-39390 series technical note, <http://www.xensor.nl>.
- [16] P. Sullivan and G. Seidel, *Phys. Rev.* **173**, 679 (1968).
- [17] Y. Kohama, C. Marcenat, T. Klein, and M. Jaime, *Rev. Sci. Instrum.* **81**, 104902 (2010).
- [18] D. Prabhakaran, A. Boothroyd, R. Coldea, and N. Charnley, *J. Cryst. Growth* **271**, 74 (2004).
- [19] R. Berthelot, D. Carlier, and C. Delmas, *Nat. Mater.* **10**, 74 (2011).
- [20] L. Viciu, J. W. G. Bos, H. W. Zandbergen, Q. Huang, M. L. Foo, S. Ishiwata, A. P. Ramirez, M. Lee, N. P. Ong, and R. J. Cava, *Phys. Rev. B* **73**, 174104 (2006).
- [21] Q. Huang, B. Khaykovich, F. C. Chou, J. H. Cho, J. W. Lynn, and Y. S. Lee, *Phys. Rev. B* **70**, 134115 (2004).
- [22] D. J. P. Morris, M. Roger, M. J. Gutmann, J. P. Goff, D. A. Tennant, D. Prabhakaran, A. T. Boothroyd, E. Dudzik, R. Feyerherm, J.-U. Hoffmann, and K. Kiefer, *Phys. Rev. B* **79**, 100103 (2009).
- [23] J. Kanter (private communication).
- [24] A. Zorkovská, M. Orendáč, J. Šebek, E. Šantavá, P. Svoboda, I. Bradarić, I. Savić, and A. Feher, *Phys. Rev. B* **72**, 132412 (2005).
- [25] M. D. Johannes, D. A. Papaconstantopoulos, D. J. Singh, and M. J. Mehl, *Europhys. Lett.* **68**, 433 (2004).
- [26] See Supplemental Material at <http://link.aps.org/supplemental/10.1103/PhysRevB.94.140402> for additional material on variation of transition temperatures in magnetic fields and temperature variation of Laue diffraction patterns for  $\text{Na}_{0.84}\text{CoO}_2$ .